Available online at www.sciencedirect.com
ScienceDirect
International Journal of Mass Spectrometry 255–256 (2006) 86–92
International Journal of Mass Spectrometry
www.elsevier.com/locate/ijms

Mass spectrometry analysis of organometallic assemblies: Bis-terpyridine-Ru(II) connectivity

Ping Wang [a], George R. Newkome [a,b], Chrys Wesdemiotis [a,*]

[a] *Department of Chemistry, The University of Akron, Akron, OH 44325-3601, USA*
[b] *Department of Polymer Science, The University of Akron, Akron, OH 44325-3909, USA*

Received 30 September 2005; received in revised form 24 February 2006; accepted 9 March 2006
Available online 24 April 2006

Abstract

Organometallic assemblies, containing the bis-terpyridinyl-Ru(II) connectivity (symbolized as [–⟨Ru⟩–]) in a range of small bismetal complexes to macrocycles possessing up to 12 metal ions, have been studied by electrospray ionization (ESI) and matrix-assisted laser desorption ionization (MALDI) mass spectrometry (MS). ESI MS is found to be a more suitable characterization method than MALDI MS, because (1) it can directly detect multiply charged ions, (2) does not alter the connectivity of the complexes through disassembly/reassembly sequences and (3) causes essentially no or very little fragmentation. Requirements for the optimum signal-to-noise ratio in ESI mass spectra include: (1) a low ionization source temperature (30 °C), (2) low skimmer voltage (10–15 V), (3) moderate flow rates of both the nebulizing and drying gases and (4) a pre-cooled sample. Tandem mass spectrometry experiments on intact complex ions indicate that the noncovalent interactions between the Ru(II) center and the two terpyridine ligands, which hold the supramolecular assembly together, are very strong.

Keywords: Organometallic polymers; ESI; MALDI; MS/MS; Noncovalent complexes

1. Introduction

Supramolecular entities contain noncovalently attached components designed to self-assemble into a defined architecture, such as those possessing star, comb or dendritic shapes [1]. Highly charged transition metal ions are often used in such species, as they can develop strong electrostatic interactions with organic ligands, leading to particularly stable assemblies. Significant efforts have been devoted in the last decade to the synthesis of supramolecular organometallic assemblies with fine-tuned physicochemical properties for specific applications [2–8]. For example, linear devices have been developed that can act as layered polyelectrolyte films, grids and photoactive molecular-scale wires, while new two- and three-dimensional species can be used for light harvesting [4,6]. X-ray crystallography and NMR spectroscopy have been the major characterization methods for these novel materials. Yet, such characterizations often pose problems because it may be difficult to generate suitable single crystals for structure determination, and/or because stereogenic problems are very challenging to solve by NMR studies [2–4,6]. Chait and co-workers [9] recognized more than 15 years ago the usefulness of electrospray ionization mass spectrometry (ESI MS) [10] for the identification of $[(bpy)_3](Ru)(Cl_2)]$ and similar transition metal complexes. Since then, ESI MS has been used for the study of a variety of organometallic systems [2,3,11–13]. A variant of ESI MS, viz. coldspray ionization mass spectrometry, was recently developed by Yamaguchi and co-workers for the targeted analysis of labile organometallics [14]. Matrix-assisted laser desorption ionization (MALDI) [15] mass spectrometry is an alternative choice for the characterization of supramolecular assemblies and polymers [5,7,16–18], although this method may coproduce misleading fragments and/or adducts that are not observed with ESI [5,7,16,17]. Here, we report a combined MS and tandem mass spectrometry (MS/MS) study of novel, Ru-based organometallic assemblies, ionized by ESI or MALDI. About 60 different organometallic complexes have been studied and 6 representative examples are discussed in detail in this paper. Both, the optimal working conditions for such systems bearing [–⟨Ru⟩–] connectivity, where ⟩– represents 2,2′:6′,2″-

* Corresponding author. Tel.: +1 330 972 7699; fax: +1 330 972 7370.
E-mail address: wesdemiotis@uakron.edu (C. Wesdemiotis).

1387-3806/$ – see front matter © 2006 Elsevier B.V. All rights reserved.
doi:10.1016/j.ijms.2006.03.006

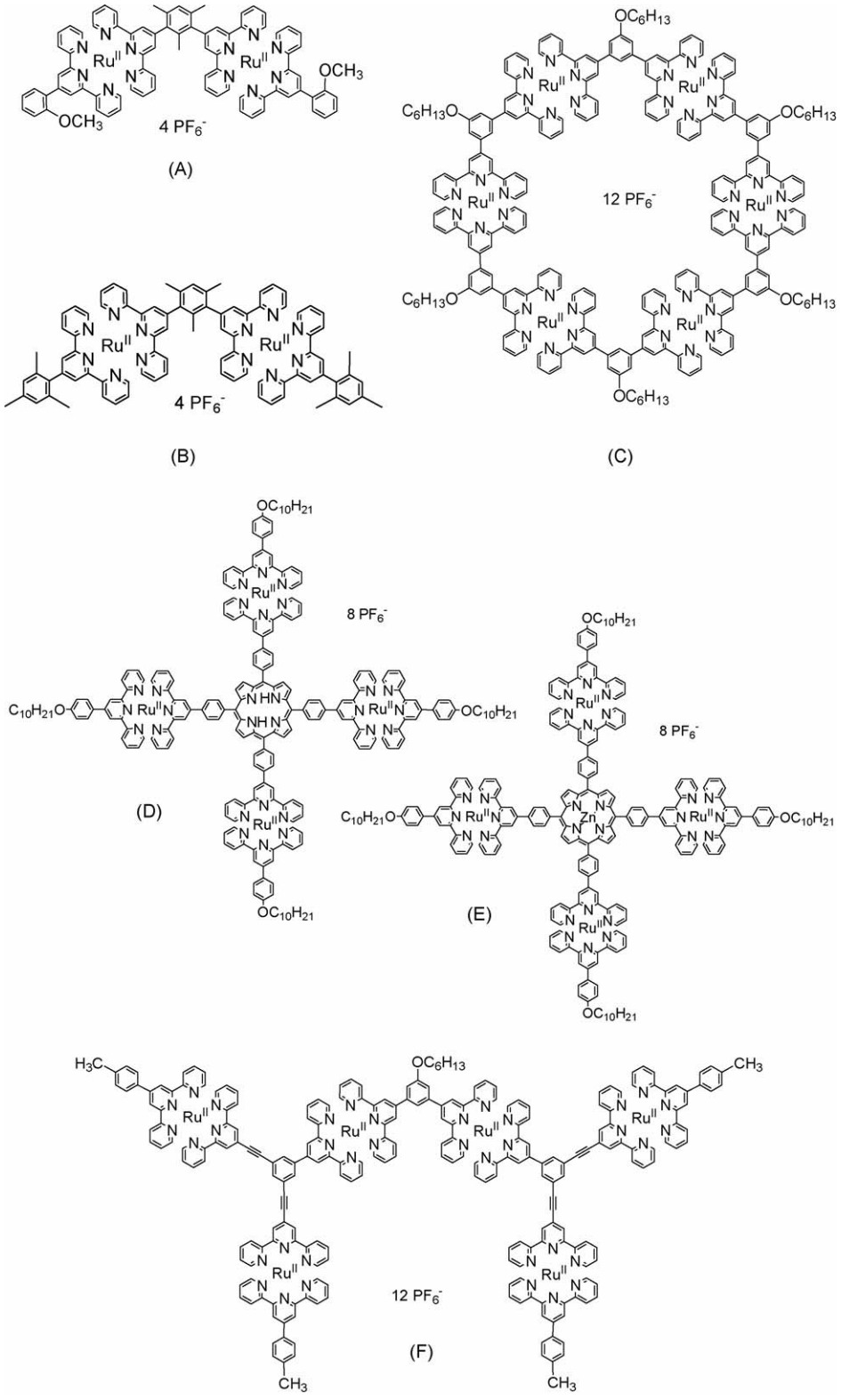

Fig. 1. Organometallic assemblies studied. Each Ru ion provides +2 charges. The positive charges of the assemblies are balanced by an equal number of PF_6^- counterions.

terpyridine, and the advantage of analyzing pre-cooled samples are demonstrated.

2. Experimental

ESI and MALDI experiments were conducted with a Bruker Esquire-LC ion trap mass spectrometer (Billerica, MA) and a Bruker Reflex III MALDI time-of-flight (ToF) mass spectrometer (Billerica, MA), respectively. The ESI solvent was either acetonitrile or chloroform. The sprayed solution was prepared by dissolving ∼1 mg of sample in 1 mL of solvent and introducing it into the ion source by a syringe pump at a rate of 100 μL/h. The spraying needle was grounded and the entrance of the sampling capillary was set at −4 kV. Nitrogen was used as the nebulizing (12–15 psi) and drying (8–12 L/min, 30 °C) gas and He as the buffer gas in the ion trap. The cone (or skimmer) voltage was held ∼10–15 V. Tandem mass spectrometry (MS/MS) experiments were performed by isolating the desired precursor ion and exciting it to decompose in the trap via collisionally activated dissociation (CAD) with the He buffer gas. The excitation (RF) amplitude was adjusted between 0.65 and 0.85 V to maximize fragment ion yield and the excitation time was set at 40 ms. In the MALDI-ToF MS experiments [19], α-cyano-4-hydroxycinnamic acid (CHCA), dithranol, 7,7,8,8-tetracyanoquinodimethane (TCNQ) and indolacrylic acid (IAA) were evaluated, as matrices. IAA gave the best signal/noise ratio and the highest abundance of quasimolecular ions for the compounds that were investigated. Solutions in acetonitrile or chloroform of the sample (10 mg/mL) and matrix (20 mg/mL) were mixed in the ratio 1:5, and the final mixture (∼0.5 μL) was deposited onto the sample holder, allowed to dry and introduced into the MALDI source. MALDI mass spectra were acquired in reflectron mode [19]. The *m/z* ratios quoted correspond to the most abundant isotope of a partially or completely resolved isotopic cluster. The synthesis of the organometallic materials studied is reported in detail elsewhere [4,6,20]. The reagents and solvents used for their MS analysis were purchased from Aldrich or Sigma (Milwaukee, WI) and were used without further purification.

3. Results and discussion

The diverse but interrelated types of organometallic assemblies [8] investigated (**A**–**F**) are shown in Fig. 1. All contain two or more [–⟨Ru⟩–] centers of connectivity with varying substitution patterns. Each Ru^{II} ion is bound to two terpyridine (tpy) moieties belonging to different ligands, with the exception of **C**, which is derived from the supramolecular assembly of a single *m*-bis-(terpyridine)benzene and $[Ru(DMSO)_4(Cl)_2]$ mixed in the ratio 1:1. The [tpy–Ru(II)–tpy] or [tpy–Ru(II)–tpy′] bonds hold the assemblies together. The organometallic assembly carries multiple positive charges, as determined by the number of Ru^{II} ions, each of which is counterbalanced by two hexafluorophosphate anions (i.e., PF_6^-). Structures **A**–**F** have been confirmed by ^{1}H NMR, ^{13}C NMR and UV/vis spectroscopy [4,6,20]. Here, we discuss their mass spectra.

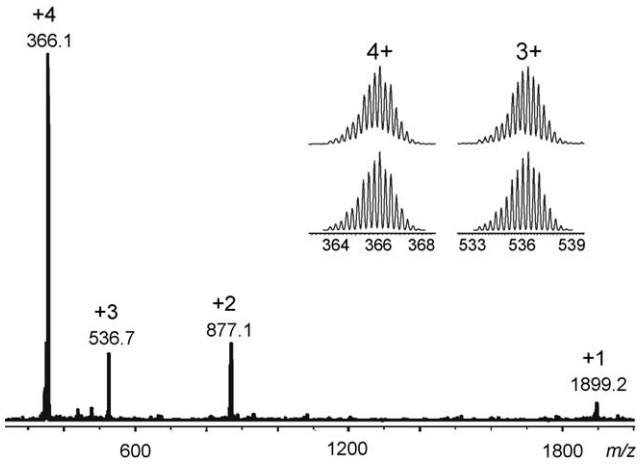

Fig. 2. ESI mass spectrum of assembly **A** (Fig. 1); the inset shows the experimental (top) and calculated (bottom) isotope patterns of the quadruply and triply charged quasimolecular ions of **A**. The numbers on top of the peaks give the charge state and the *m/z* value of the most abundant isotope.

3.1. MS and MS/MS studies of small organometallic assemblies *A* and *B*

Fig. 2 depicts the ESI mass spectrum of the small bismetal assembly **A**, obtained with the drying gas temperature normally used (300 °C) and with a low skimmer voltage (∼10 V instead of the commonly used 60 V). The assembly is observed as a quadruply charged quasimolecular ion as well as with +3, +2 and +1 charges. The three latter charge states contain one, two, and three PF_6^- anions, respectively. The inset in Fig. 2 shows an expanded view of the measured (top) and predicted (bottom) isotopic patterns for the quadruply and triply charged ions; the experimental and theoretical patterns match perfectly. The quasimolecular ions of **A** were also analyzed by MS/MS (CAD), in order to gain information about the fragmentation behavior in such ruthenium connectivity. The MS/MS spectrum of the singly charged ion, Fig. 3(a), contains fragments from consecutive losses of HPF_6; up to three occur, which is consistent with the three PF_6^- units present in this charge state. Each HPF_6 loss is accompanied by a competitive PF_5 elimination ($PF_6^- \rightarrow PF_5 + F^-$), proceeding in

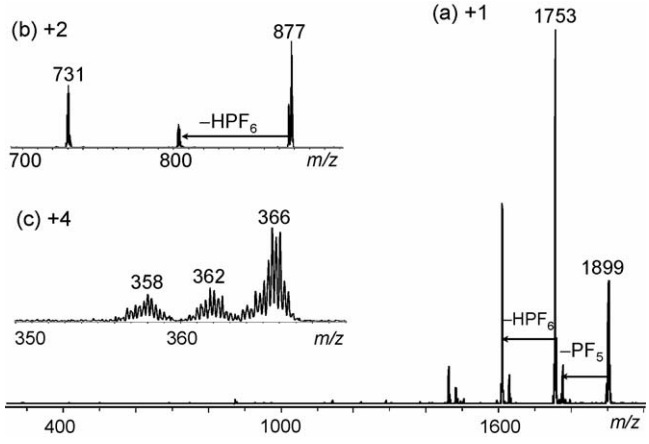

Fig. 3. MS/MS (CAD) tandem mass spectra of (a) singly, (b) doubly and (c) quadruply charged **A**. The numbers on top of the peaks give *m/z* values.

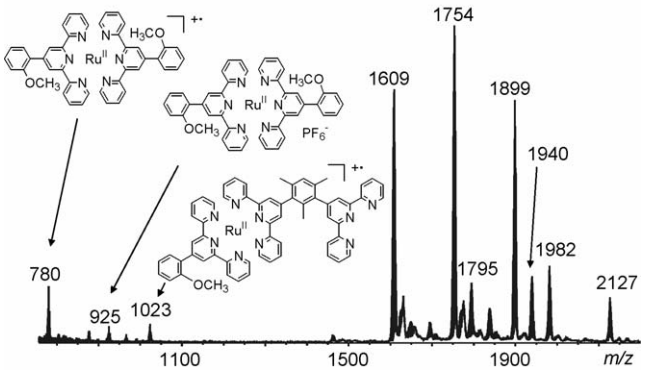

Fig. 4. MALDI-ToF mass spectrum of assembly **A**. The broad peaks between the isotope-resolved signals arise from post-source decay of higher-mass ions (i.e., fragmentations after the ions have exited the ion source [19]). The structures in the insets correspond to the ions marked by the arrows (see text).

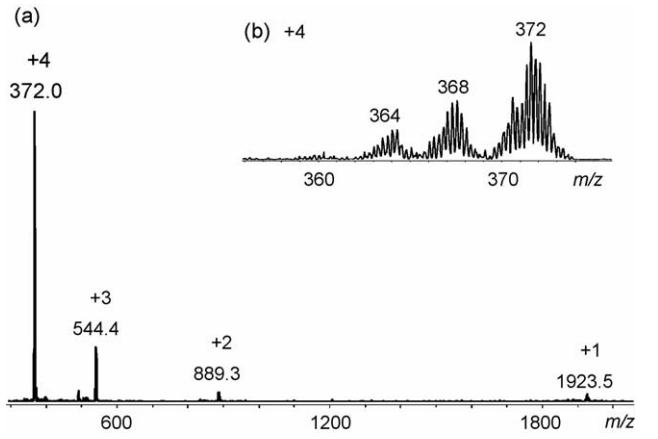

Fig. 5. (a) ESI MS and (b) ESI MS/MS (CAD) (quadruply charged) mass spectra of assembly **B**. The numbers on top of the peaks give *m/z* values.

much lower yield. For each loss of HPF_6, proton abstraction from the organic ligands occurred. These protons are most probably derived from the central aryl $–CH_3$ or $–OCH_3$ substituents. The resulting anions may increase (through resonance) the charge density at the N atoms coordinated to Ru^{II}, leading to stronger ligand–metal bonds [4,6]. It is noteworthy that dissociation of the noncovalent Ru^{II}–tpy bonds is not observed, indicating that they are stronger than the Ru^{II}/PF_6^- interactions.

Fig. 3(b) shows the MS/MS spectrum of the doubly charged quasimolecular ion, which decomposes solely via consecutive losses of HPF_6. A similar reactivity is observed for the +3 charge state (one HPF_6 loss). Finally, the quadruply charged ion, which lacks PF_6^- counterions, undergoes H_2, CH_4 and CH_3OH losses, cf. Fig. 3(c); these dissociations presumably take place at the $–CH_3$ and $–OCH_3$ groups. Cleavages at the Ru^{II}–tpy bonds do not occur, demonstrating once more the strong interaction between metal ion and ligands.

Fig. 4 shows the MALDI-ToF mass spectrum of assembly **A** using IAA as matrix. Only singly charged ions are observed in this spectrum. The peak at *m/z* 1899 is the assembly **A** with one less PF_6^- (145 u). The product at *m/z* 1754 is missing two PF_6 units, while that at *m/z* 1609 lacks three such units; these ions still contain one (*m/z* 1609) or two (*m/z* 1754) PF_6^- counterions. Note that the overall charge state is +1, because the removal of n PF_6^- anions is accompanied by the addition of $n-1$ electrons [7]. The plume of charged particles created in the MALDI process contains highly charged clusters as well as electrons [21]. Electron capture by initially formed high charge states (>1) causes partial neutralization, yielding the observed singly charged ions. Ions with one charge survive the longest in the plume and, thus, only these species are ultimately detected in the spectra [5,7,16–18]. For most analytes, such electron capture results in dissociation; the Ru^{II}/tpy assemblies, however, can be reduced to resonance-stabilized radicals that are particularly stable and, hence, detectable as intact complexes.

The three most abundant peaks in the lower *m/z* range of the MALDI mass spectrum, viz. *m/z* 780, 925 and 1023 (Fig. 4), agree well with the smaller assemblies shown as insets. These products most likely originate from prompt fragmentation (i.e., fragmentation during the MALDI event [19]) of the assemblies at *m/z* 1609 and 1754. There are several ions in the high-mass end of the spectrum, including *m/z* 1795, 1940, 1982 and 2127, which could not be identified conclusively. These ions may be formed during sample preparation or/and the ionization process. Studies are under way to determine their origin [22].

Assemblies **A** and **B** only differ in the side chains of the peripheral ligands. It is therefore not surprising that they behave similarly under ESI conditions. Fig. 5(a) shows the ESI mass spectrum of **B**, which contains quadruply, triply, doubly and singly charged quasimolecular ions. The inset (Fig. 5(b)) is the MS/MS spectrum of the quadruply charged **B**, revealing consecutive dissociations of CH_4. Again, ligand detachment is not observed. The MALDI-ToF mass spectrum of **B** (Fig. 6) is quite similar to that of assembly **A**, with peaks at *m/z* 1923 (assembly **B** with one less PF_6^-), *m/z* 1778 (from elimination of a second PF_6^-, followed by electron capture) and *m/z* 1633 (after a further PF_6^- loss/electron capture). The ions at *m/z* 804 and 949 are the reassembled complexes shown in the insets and probably arise by consecutive fragmentation of *m/z* 1633 or 1778. Larger, unidentified products are observed as well, appearing at *m/z* 1819, 1964, 2006 and 2151 [23]. The ESI and MALDI results for **A** and **B** clearly demonstrate that ESI MS provides

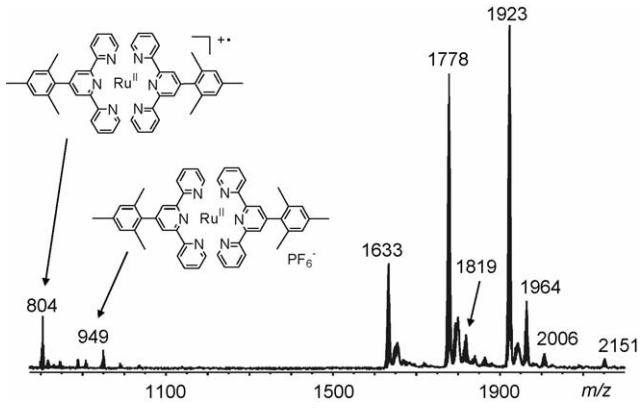

Fig. 6. MALDI-ToF mass spectrum of assembly **B**. The broad peaks between the isotope-resolved signals arise from post-source decay of higher-mass ions (i.e., fragmentations after the ions have exited the ion source [19]). The structures in the insets correspond to the ions marked by the arrows (see text).

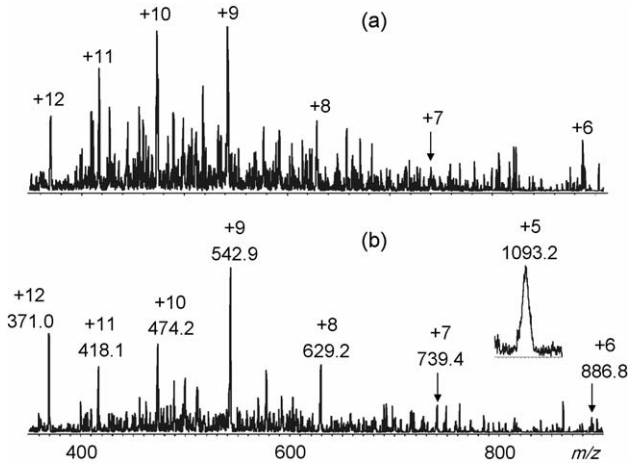

Fig. 7. ESI mass spectrum of assembly **C** acquired with the drying gas at room temperature and low skimmer voltage (see text), using (a) a sample solution at room temperature or (b) a sample solution pre-cooled to −8 °C. The inset shows the peak for a lower-charge state, detected separately over a narrow mass range. The numbers on top of the peaks give the *m/z* value and charge state of the most abundant isotope.

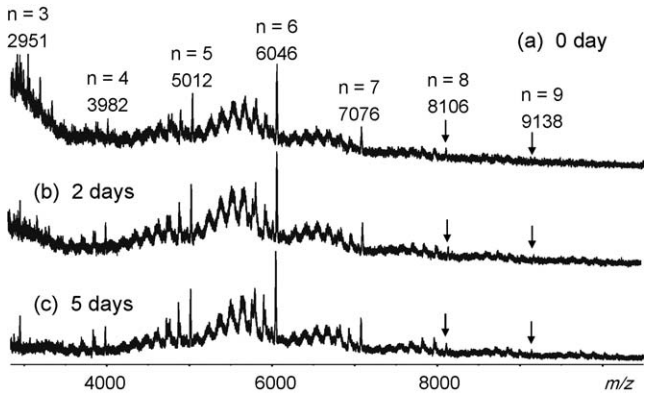

Fig. 8. MALDI-ToF mass spectrum of assembly **C**, acquired from (a) a fresh solution of **C** and the same solution after it stood for (b) 2 or (c) 5 days at room temperature. The peaks labeled by *m/z* values correspond to singly charged quasimolecular ions of $[(tpy)_2(Ru)(PF_6)_2]_n$ ($n = 3$–9) assemblies, having the composition [assembly − PF_6^-]$^+$. The broad peaks at the lower *m/z* side of the quasimolecular ions arise from post-source decay.

a more straightforward characterization of such organometallic assemblies, whereas MALDI-ToF MS causes association and dissociation reactions that compromise spectral interpretation.

3.2. ESI and MALDI MS studies of larger assemblies *C*, *D*, *E* and *F*

Mass spectrometry characterization of the larger supramolecular organometallic assemblies, which usually carry more charges, becomes challenging. For example, if sample **C** is analyzed under the same conditions as samples **A** and **B**, no useful spectra can be obtained (only background noise is detected). This led us to determine that low drying gas temperature and low skimmer voltage are critical in these cases. The ESI mass spectrum of **C** depicted in Fig. 7(a) was acquired with the drying gas temperature set at 30 °C and with a low skimmer voltage (∼10 V). The flow rates of the nebulizing and drying gases were also adjusted higher than in normal operation, viz. at 15 psi versus 10 psi (nebulizing) and at 12 L/min versus 8 L/min (drying gas), to minimize heating of the ions during their transport to the mass analyzer. Since room temperature is the lowest temperature accessible with our ESI ion trap, an alternative means to remove excess energy that could cause sample deterioration during the ESI process is to pre-cool the sample solution. When the sample solution is stored in the freezer (−8 °C) for at least 12 h before analysis, the spectrum of Fig. 7(b) is obtained for **C**, which has a markedly better signal-to-noise ratio. Thus, sample pre-cooling is one extra step for getting enhanced mass spectral data from these large supramolecular organometallic assemblies. The most abundant peaks in the resulting spectra always correspond to ions with relatively high (but not the highest) charge states, which appear at lower mass-to-charge values. In order to detect peaks of higher *m/z* with fair intensity, a narrow range around the predicted *m/z* must be scanned and the scanning parameters should be adjusted accordingly.

Assembly **C** was also subjected to MALDI-ToF MS analysis using IAA as matrix, cf. Fig. 8(a). Unlike the corresponding ESI mass spectrum (Fig. 7), which was dominated by differently charged quasimolecular ions of the hexagon-like structure **C**, the major peaks in the MALDI mass spectrum correspond to singly charged ions from $[(tpy)_2(Ru)(PF_6)_2]_n$ complexes ($n = 3$–9), containing n bis(terpyridine) moieties, n Ru^{II} ions and $2n - 1$ PF_6^- counterions. Because of the 120°-angle between the terpyridine units, only the hexameric complex ($n = 6$) can have a strain-free cyclic structure (shown in Fig. 1), suggesting that the other complexes observed in the MALDI mass spectrum are either ring-opened, horseshoe-like ($n \leq 5$) species or/and less stable, strained macrocycles ($n \geq 7$). The same sample solution was analyzed by MALDI-ToF MS also after standing at room temperature for 2 or 5 days, cf. Fig. 8(b and c). There is no dramatic change vis-à-vis the spectrum of the fresh sample, Fig. 8(a), even when the sample solution is pre-cooled or the matrix changed (spectra not shown), indicating that the partial disassembly of cyclic structure **C** and the formation of the larger macrocycles takes place during the MALDI event and not upon sample preparation. The MALDI mass spectra also show a considerable degree of metastable fragmentation (broad peaks [19]), presumably because a significant amount of internal energy is deposited in the desorption/ionization step. These results point out that MALDI-ToF MS is inferior, compared to ESI MS, for the analysis of self-assembling complexes analogous to those studied here.

In contrast to **C**, assembly **D** is composed of difference subunits, viz. small peripheral ligands (similar to those in **C**) and a large porphyrin derivative centerpiece. Replacing the two protons in the center of the porphyrin ring of assembly **D** with a Zn(II) ion yields assembly **E**. Fig. 9 depicts the ESI mass spectra of assemblies **D** and **E**. The highest charge states observed, +8, contain no PF_6^- counterions. These, together with all other, less charged quasimolecular ions provide definitive identification of the corresponding assemblies. Fig. 10 shows the MALDI mass spectra for pre-cooled (−8 °C) complexes **D** and **E**. The ion at

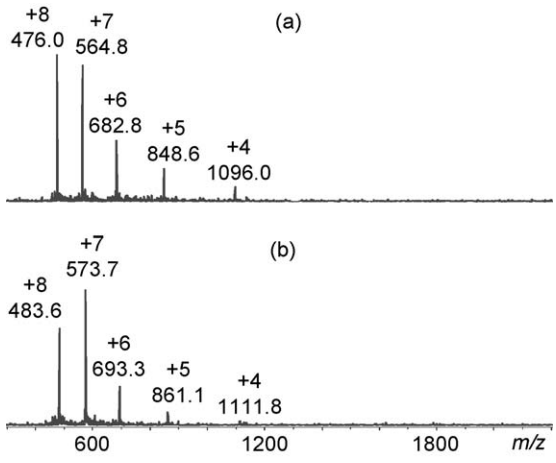

Fig. 9. ESI mass spectra of assemblies (a) **D** and (b) **E** acquired using a pre-cooled sample (−8 °C) and low drying gas temperature and skimmer voltage. The numbers on top of the peaks give the charge state and the *m*/*z* value of the most abundant isotope.

m/*z* 4819 in Fig. 10(a) is $[\mathbf{D} - PF_6^-]^+$, i.e., the quasimolecular ion with one PF_6^- less than the complete assembly (Fig. 1). The following three peaks arise from complexes that have lost 1–3 additional PF_6^- units upon MALDI, as explained for assemblies **A** and **B**; each PF_6^- loss is accompanied by electron capture and lowers the mass by 145 u while maintaining a +1 charge. The ion at *m*/*z* 4881 in Fig. 10(b) corresponds to $[\mathbf{E} - PF_6^-]^+$, i.e., the complete assembly **E** (Fig. 1) less one PF_6^- counterion. Below *m*/*z* 3000, the same ions are observed from **D** and **E**, but with different relative intensities. These products, probably fragments, have not yet been identified.

Assembly **F** is a branched assembly composed of three different subunits. Pre-cooling of sample **F** leads to an ESI mass spectrum (Fig. 11), containing a series of variously charged quasimolecular ions. Fig. 12 is the MALDI-ToF mass spectrum of the same pre-cooled (−8 °C) assembly **F**, in which only small complexes are detected (indicated in the insets). The observed ions appear to be fragments, arising from highly charged assemblies that underwent electron capture in the MALDI plume (vide supra). Once again, our results point out that ESI MS is more suitable than MALDI MS for the nondestructive analysis of this type of organometallic assemblies.

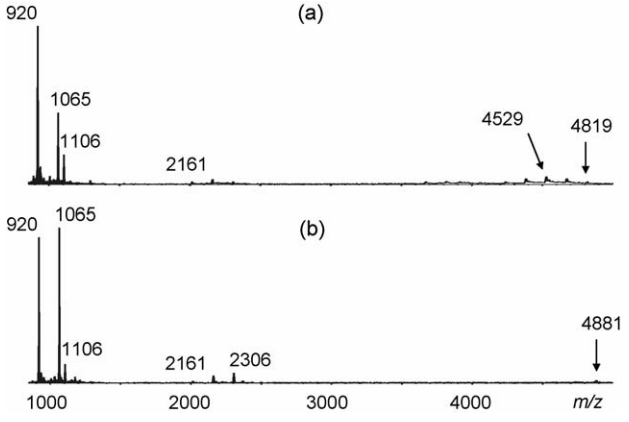

Fig. 10. MALDI-ToF mass spectra of assemblies (a) **D** and (b) **E** acquired using pre-cooled samples.

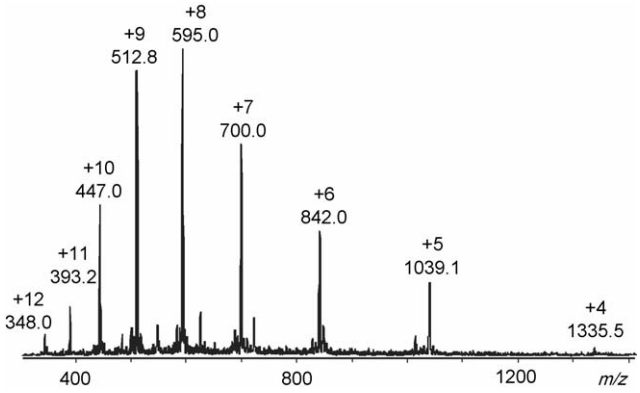

Fig. 11. ESI mass spectrum of assembly **F** acquired using a pre-cooled sample (−8 °C) and low drying gas temperature and skimmer voltage. The numbers on top of the peaks give the charge state and the *m*/*z* value of the most abundant isotope.

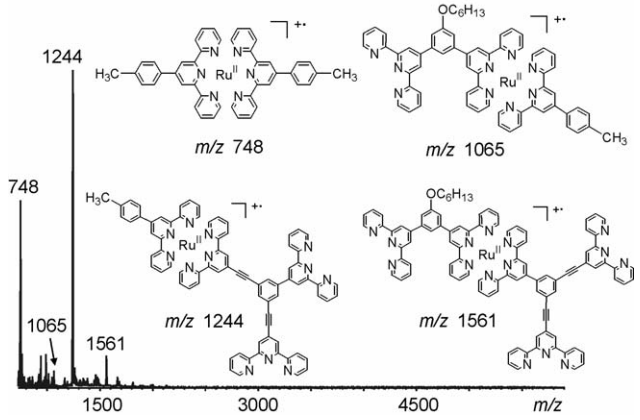

Fig. 12. MALDI-ToF mass spectrum of assembly **F** acquired from a pre-cooled sample. The structures of the ions labeled in the spectrum are given in the insets.

4. Conclusions

In summary, ESI MS is more suitable than MALDI MS for the characterization of Ru^{II}/tpy-based supramolecular organometallic assemblies held together by electrostatic (noncovalent) interactions.

The optimized conditions for ESI analysis of such assemblies are low ionization source temperature (30 °C), low skimmer voltage (∼10 V), moderate flow rates of nebulizing gas and drying gas and a pre-cooled sample; the latter condition is very important for the best possible signal-to-noise ratio (and, hence, detection sensitivity) in the resulting mass spectra.

Pre-cooling removes some of the vibrational excitation of the organometallic assemblies, making it more probable that the corresponding quasimolecular ions generated upon ESI reach intact the ion trap for their mass (and MS/MS) analysis. The best possible spectra are obtained within ∼30 min after removal of the sample from the freezer. From the complexes discussed

in this paper, the cyclic construct **C** leads to a noticeably noisier mass spectrum than the other, linear assemblies. A possible cause for this difference is the collisional reactivation that can occur when the ions are transported from ambient pressure to the ion trap. The cyclic structure should have a higher collisional cross-section and, thus, would be more susceptible to destruction en route to the mass analyzer.

MALDI generally deposits more internal energy than ESI. In fact, the post-source decay (PSD) mass spectra acquired in reflectron MALDI-ToF instruments are the result of the considerable internal energy distributions that can be transferred in the MALDI event [19]. The internal energy added upon MALDI appears to outweigh any vibrational cooling effected by freezing of the sample, thus causing extensive or complete fragmentation of the assemblies. The relative abundance of the singly charged quasimolecular ion (i.e., of [assembly $-\ PF_6{}^-]^+$) in the MALDI mass spectra varies with the matrix used, increasing in the order IAA > dithranol > TCNQ (or other matrices). Based on the latter trend, matrix acidity is not detrimental. The UV spectrum of a cyclic complex similar to **C** ($-CH_3$ instead of $-OC_6H_{13}$ side chains) contains band maxima at 290, 312 and 496 nm. The band at 312 nm is near but not in resonance with the light emitted by the MALDI laser (337 nm). Hence, the samples analyzed might absorb weakly the laser light, which in turn could contribute to the large degree of prompt fragmentation observed in the MALDI-ToF mass spectra.

Acknowledgements

We thank Dr. Pingshan Wang, Dr. Tae Joon Cho, Dr. Carol Shreiner and Sinan Li for the synthesis of the analyzed samples, and Dr. Kathleen M. Wollyung for experimental assistance. We acknowledge generous financial support from the National Science Foundation [CHE-0517909 (CW) and DMR-0401780 (GRN)].

References

[1] J.-M. Lehn, Supermolecular Chemistry: Concepts and Perspectives, VCH, Weinheim, 1995.
[2] C. Moucheron, A. Kirsch-De Mesmaeker, A. Dupont-Gervais, E. Leize, A. Van Dorsselaer, J. Am. Chem. Soc. 118 (1996) 12834.
[3] J.W. Kriesel, S. König, M.A. Freitas, A.G. Marshall, J.A. Leary, T.D. Tilley, J. Am. Chem. Soc. 120 (1998) 12207.
[4] G.R. Newkome, T.J. Cho, C.N. Moorefield, G.R. Baker, R. Cush, P.S. Russo, Angew. Chem. Int. Ed. 38 (1999) 3717.
[5] M. Zhou, J. Roovers, Macromolecules 34 (2001) 244.
[6] G.R. Newkome, T.J. Cho, C.N. Moorefield, R. Cush, P.S. Russo, L.A. Godinez, M.J. Saunders, P. Mohapatra, Chem. Eur. J. 8 (2002) 2946.
[7] H. Hofmeier, P.R. Andres, R. Hoogenboom, E. Herdtweck, U.S. Schubert, Aust. J. Chem. 57 (2004) 419.
[8] U.S. Schubert, H. Hofmeier, G.R. Newkome, Modern Terpyridine Chemistry, Wiley–VCH, Weinheim, 2006.
[9] V. Katta, S.K. Chowdhury, B. Chait, J. Am. Chem. Soc. 118 (1990) 12834.
[10] M. Yamashita, J.B. Fenn, J. Phys. Chem. 88 (1984) 4451.
[11] C.A. Schalley, T. Müller, P. Linnartz, M. Witt, M. Schäfer, A. Lützen, Chem. Eur. J. 8 (2002) 3538.
[12] P.J. Dyson, J.S. McIndoe, Inorg. Chim. Acta 354 (2003) 68.
[13] R. Zadmard, A. Kraft, T. Schrader, U. Linne, Chem. Eur. J. 10 (2004) 4233.
[14] S. Sakamoto, M. Fujita, K. Kim, K. Yamaguchi, Tetrahedron 56 (2000) 955.
[15] M. Karas, D. Nachmann, U. Bahr, F. Hillenkamp, Int. J. Mass Spectrom. Ion Processes 78 (1987) 53.
[16] U.S. Schubert, C. Eschbaumer, Polym. Prepr. 41 (1) (2000) 676.
[17] M.A.R. Meier, B.G.G. Lohmeijer, U.S. Schubert, J. Mass Spectrom. 38 (2003) 510.
[18] D. Joester, V. Gramlich, F. Diederich, Helv. Chim. Acta 87 (2004) 2896.
[19] R.C. Cotter, Time-of-Flight Mass Spectrometry: Instrumentation and Applications in Biological Research, ACS Professional Reference Books, Washington, DC, 1997.
[20] G.R. Newkome, P.S. Wang, S.-H. Hwang, Polym. Prepr. 46 (2005) 1119.
[21] M. Karas, M. Glückmann, J. Schäfer, J. Mass Spectrom. 35 (2000) 1.
[22] The *m/z* 2127 ion in Fig. 4 is consistent with the composition $[\mathbf{A} - PF_6 + CH_3CN + IAA]^+$, *m/z* (1899 + 41 + 187) = 2127. The ions at *m/z* 1982, 1940 and 1795 can arise from *m/z* 2127 via eliminations of PF_6 (145 u) and IAA (187 u). MALDI-CAD experiments are in progress to verify these suppositions. Expectedly, the peaks at *m/z* 1795, 1940, 1982 and 2127 disappear while other, new adducts and their fragments appear, when the matrix is changed to dithranol.
[23] The *m/z* 2151 ion in Fig. 6 is consistent with the composition $[\mathbf{B} - PF_6 + CH_3CN + IAA]^+$, *m/z* (1923 + 41 + 187) = 2151. The ions at *m/z* 2006, 1964 and 1819 can arise from *m/z* 2151 via eliminations of PF_6 (145 u) and IAA (187 u). MALDI-CAD experiments are in progress to verify these suppositions. Expectedly, the peaks at *m/z* 1819, 1964, 2006 and 2151 disappear while other, new adducts and their fragments appear, when the matrix is changed to dithranol.